

α_s DEPENDENCE IN THE EQUILIBRATION IN RELATIVISTIC HEAVY ION COLLISIONS

S.M.H. Wong

Fachbereich Physik, Universität Wuppertal, D-42097 Wuppertal, Germany

The dependence of the equilibration of the parton plasma on the value of the strong coupling is studied in Au+Au collisions at LHC and at RHIC energies. With increasing coupling, the following are found to happen: 1) both thermal and chemical equilibration speed up, 2) in the final degree of equilibration, only quarks and antiquarks show obvious improvements but not gluons and 3) the plasma cools much more rapidly. The deconfinement phase transition will therefore takes place sooner and it naturally results in the shortening of the parton phase of the plasma. The exact duration of this phase is however sensitive to the value of the coupling. A change from $\alpha_s = 0.3$ to $\alpha_s = 0.5$, for example, reduces the lifetime of the parton phase at LHC by as much as 4.0 fm/c. The total generated entropy is another sensitive quantity to the coupling. Larger values of α_s will lead to entropy reduction and therefore reduction both in the duration of the mixed phase, assuming there is a first order deconfinement phase transition, as well as in the final pion multiplicity. It is shown that the common choice of $\alpha_s = 0.3$ is not a good value for the entire duration of the evolution given that the system undergoes substantial changes from the beginning to the time that the deconfinement phase transition is about to take place assumed to be at $T_c \sim 200$ MeV. Instead, by using a more consistent simple recipe, the system is allowed to decide its own strength of the interactions which evolves with the system as it should. With this approach, α_s increases with time and this leads to acceleration in the equilibration even as equilibrium is near. This is opposite to the behavior of the equilibration of a molecular gas or ordinary many-body system where the interaction strength is fixed. In such system, the net interactions will slow down as the system is near equilibrium.

WU B 97/13 (to appear in Phys. Rev. C)

I. INTRODUCTION

With the asymptotic freedom of QCD, one expects quarks and gluons to behave almost as free particles at very high energies and under extreme conditions. Such extreme conditions as believed to be found in the early universe can, to a limited extent, be recreated in the laboratories in the experiments of heavy ion collisions. As highly energetic and relativistic matter collides at 200 GeV/A at RHIC and 6.3 TeV/A at LHC, nucleons lose their individual identities in favor of a gas of partons. A main goal of the experiments is to establish beyond doubt the existence of this parton plasma. In order to do so, distinctive signs in the guise of particle signatures must be looked for. Numerous works have already been devoted to these. Also of importance is the temporal development of the parton plasma which directly influences the various particle signatures. In our previous investigation into the equilibration of this QCD plasma [1,2], we have shown that, as in agreement with previous works [3–6], chemical equilibration in the partonic mixture cannot be completed by the time that the deconfinement phase transition sets in. However, we also pointed out that kinetic equilibration might also not be as quick, or perhaps one should say, not as perfectly equilibrated as one would have liked. A thermalization time within 1.0 fm/c is unrealistic as shown in [4,5]. It was pointed out in [7] that very fast equilibration for gluons, at least, based on estimate of the transverse energy deposited in the central collision region, might be possible depending on what parton distribution was used. However, one should be wary of the fact that initially the matter is highly compressed, so even though thermalization may approximately be achieved, the expansion may drive it out of equilibrium. The question then is whether this gluon early thermalization, if it can be achieved, is a transient or a maintainable thermalization. We have shown that in our previous work [1,2], expansion can indeed drive out the early thermalization which is to be recovered progressively only later.

Unlike in a vacuum, in a dense QCD medium, collective effects will provide for infrared screening [8,9] and so we have no need for an arbitrary soft momentum cutoff. This feature reduces the dependency of our investigation on the number of external parameters. And in fact, apart from the obvious initial inputs, the only remaining variable which one has a certain freedom to choose is α_s . Since after all, we are doing a perturbative calculation, a small $\alpha_s = 0.3$ was chosen, which corresponds to an average momentum transfer of $Q \sim 2.0$ GeV and $\Lambda_{QCD} \sim 200$ MeV. One can see from previous works on chemical equilibration [5,6,10], particle production reduces the temperature T and this lasts over several fm/c during which T drops by several hundreds of MeV. Consequently, the average parton energy

also varies considerably. As a result, we do not and cannot expect the average momentum transfer to remain at around $Q \sim 2.0$ GeV. Therefore α_s should also vary during the equilibration and evolution of the parton plasma. This effect has not been taken into account. If thermalization is very fast, one can perhaps argue for a roughly constant α_s during thermalization but certainly not during chemical equilibration when the system changes considerably. We have plotted in Fig. 1, the average parton energies for quarks and gluons during the evolution of the plasma in our previous investigation [2]. As can be seen, assuming the average momentum transfer is of the order of the average parton energy, $Q \sim \epsilon/n$, one can neither expect Q to stay at around 2.0 GeV at LHC nor at RHIC. We therefore investigate the dependence of our previous results on equilibration on α_s . This we carry out in two ways. The first is to use various fixed α_s and the second is to use an α_s determined by the system. The later approach means we do not choose a value for α_s but let the system decides what it should be. Since the system is evolving, the resulting coupling will evolve with the system. These will be explained in the following sections.

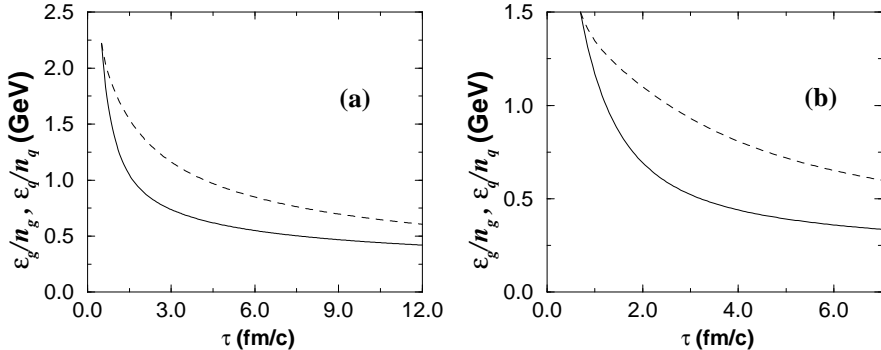


FIG. 1. The evolution of the average parton energy of gluon (solid line) and quark or antiquark (dashed line) at (a) LHC and (b) RHIC with $\alpha_s = 0.3$.

In Sec. II, we recapitulate briefly our method and basic equations. We comment on the questions related to the possible inclusion of a mean field term and possible role played by instabilities. What values to use for α_s in our investigation and how to obtain an evolving coupling are explained. In Sec. III, results on the effect of α_s on the equilibration will be shown and consequences discussed. We then show that a plasma governed by QCD is no ordinary many-body system.

II. THE EVOLUTION EQUATIONS

Quantum effects have proved so far to be hard to include in all its details [11–18] and interference in many particle interactions are largely absent (except in a limited sort of way in Eq. (6) below). One can at best, at present, to investigate the equilibration in heavy ion collisions in its full form by semi-classical means.

Our basic equation is the Boltzmann equation which can, in Baym's manner [19], be rewritten as

$$\frac{\partial f_i}{\partial \tau} \Big|_{p_z \tau} = C_i(p_\perp, p_z, \tau) \quad (1)$$

$i = g, q, \bar{q}$, by the assumption of one-dimensional boost invariant longitudinal expansion in the very central region of the collision of two highly relativistic heavy ions. The collision terms C_i on the right hand side include sums over all relevant interactions and we approximate it by the relaxation time approximation, which is expedient for our purpose and has been used in simpler studies of thermalization [20–23]. Explicitly, it is written in the form

$$C_i(p_\perp, p_z, \tau) = -\frac{f_i(p_\perp, p_z, \tau) - f_{eq\,i}(p_\perp, p_z, \tau)}{\theta_i(\tau)} \quad (2)$$

where f_{eq} is the full equilibrium distribution and is a function of the equilibrium temperature T_{eq} . Because we are considering an expanding system, this approximation is not sufficient to close the equations. T_{eq} and θ remain functions of time. In any case, we need input from QCD which is obtained by explicitly constructing C_i also from QCD interactions [1,2]. We use the same set of interactions as before

$$gg \longleftrightarrow ggg, \quad gg \longleftrightarrow gg, \quad (3)$$

$$gg \longleftrightarrow q\bar{q} , \quad gg \longleftrightarrow gq , \quad g\bar{q} \longleftrightarrow g\bar{q} , \quad (4)$$

$$q\bar{q} \longleftrightarrow q\bar{q} , \quad qq \longleftrightarrow qq , \quad \bar{q}\bar{q} \longleftrightarrow \bar{q}\bar{q} . \quad (5)$$

The collision terms are constructed from the well known vacuum matrix elements of the above interactions at leading order in α_s [24] but rendered infrared safe by medium screening. These screening effects are put in by hand in terms of the Debye screening and quark medium mass. They are calculated from the distributions f_i and are therefore functions of α_s as well as τ . Admittedly, they are only part of the screening effects since they have no momentum dependence. But for our purpose, they are sufficient to provide the right order of magnitude for the screening. With these α_s dependent masses, the collision terms become more complicated functions of α_s . The explicit form of the infrared screened matrix elements can be found in [1,2]. Apart from screening, other medium effect will also have to be included, that is the Landau-Pomeranchuk-Migdal (LPM) suppression of gluon radiations or absorptions due to multiple interactions. This is partially incorporated in the two to three gluon multiplication collision term in the form of a theta function [25–27]. This collision term as appeared in the collision entropy rate per unit volume is

$$\left(\frac{\partial s_g}{\partial \tau} \right)_{coll}^{gg \longleftrightarrow ggg} = \frac{1}{4} (2\pi)^4 \nu^2 \prod_{i=1}^5 \frac{d^3 \mathbf{p}_i}{(2\pi)^3 2p_i^0} |\mathcal{M}_{gg \rightarrow ggg}|^2 \delta^4(p_1 + p_2 - p_3 - p_4 - p_5) \ln \left(\frac{f_1 f_2 (1 + f_3)(1 + f_4)(1 + f_5)}{(1 + f_1)(1 + f_2)f_3 f_4 f_5} \right) \times [f_1 f_2 (1 + f_3)(1 + f_4)(1 + f_5) - f_3 f_4 f_5 (1 + f_1)(1 + f_2)] \theta(\Lambda - \tau_{QCD}) . \quad (6)$$

where Λ is the gluon mean free path, $\tau_{QCD} = \sqrt{s}(p_1 + p_2) \cdot p_5 / (4p_1 \cdot p_5 p_2 \cdot p_5)$ is the gluon formation time of the radiated gluon with momentum p_5 and $s = 2p_1 \cdot p_2$ is the squared of the centre-of-momentum energy of the parent gluons. The gluon mean free path is a function of α_s as well as the Debye screening mass [1,6]. The resulting dependence on α_s of this is more complicated than the binary interaction terms. Combining these explicit collision terms and that of the relaxation time approximation, one can solve for $T_{eq,i}$ and θ_i at each instance in time and hence the f_i distributions which depend on this two variables can be determined.

As we explained briefly in our previous works [1,2], our $f_{eq}(\tau)$ is the momentary “target” equilibrium distribution at which the particle distribution of the system will eventually settle, if one is able to stop the expansion at τ . This can be seen in the analytic form of the solution to the approximation Eq. (4) in [2]. At large time compared to θ , the solution is dominated by the second term and the integrand in this term is dominated by the upper limit of the integral. One can approximate the integral by evaluating the integrand at the peak and multiply by the “width” of this peak, which is approximately given by θ . This means that the solution will tend to the equilibrium distribution at large times. Therefore one should not confuse our approach with the Chapman-Enskog method of linearizing the Boltzmann equation. In fact, the linearization of this method does not give a collision term of the simple form of the relaxation model. Also the leading particle distribution of the Chapman-Enskog expansion does not have the same physical meaning as our f_{eq} . In the Chapman-Enskog case, the leading distribution is the best fitted local distribution to the system at any moment in line with the locally equilibrated hydrodynamical description of the method but ours is rather what the system would at any time like to reach and we try to describe what will happen early on in relativistic heavy ion collisions and therefore before the hydrodynamic expansion phase. The collision model by itself contains no information about QCD, but because it is taken to model the collision terms and so can be equated to the latter for fixing the parameters of the distribution.

At this point, we would like to comment on the lack of a mean field term in our basic equation Eq. (1) which is often a point of criticism. In [28,29], it was shown that unstable collective plasma modes might develop via chromoelectromagnetic mean fields when the particle momentum distribution is anisotropic. Anisotropy will no doubt be featured in the early stage of heavy ion collisions which may give rise to instabilities. As worked out in [28,29], the time scales of the instabilities are earlier than our initial time τ_0 both at LHC and at RHIC. Therefore these instabilities will influence our initial inputs. They then become part of the many uncertainties associated already with the initial conditions. Their effects on the equilibration can then be studied as part of the initial condition dependence. By the time that the evolution starts, collisions are important and the derivations in [28,29] are no longer applicable. In any case, the mean field term in the Vlasov-Boltzmann equation does not generate entropy and without collisions, the mean field term cannot bring about equilibration. Therefore we are doubtful that it can be very important for equilibration in a direct way. It may have some indirect effects as suggested in [28] but that needs further studies to clarify.

To study the dependence of equilibration on α_s , we evolve the plasma using other values. The previous results were obtained with $\alpha_s = 0.3$. In order to make the effects prominent and unambiguous, we choose $\alpha_s = 0.5$ and $\alpha_s = 0.8$. With such large α_s and in particular $\alpha_s = 0.8$, one can no longer trust leading order calculations, our aim is to make the influence of α_s manifest. In any case, we are not after quantitative but qualitative results. Apart from these values, as mentioned in the introduction and shown in Fig. 1, the average parton energies vary over a rather

large range during the evolution and so also should the momentum transfers. To complete this study, we then use a coupling which evolves with the system. This is done by using the following recipe. Since two colliding partons each carrying the average parton energy will have a maximum momentum transfer equals to twice the average parton energy so we can assume the average transfer is of the order of the average parton energy

$$Q \sim <\epsilon_g + \epsilon_q + \epsilon_{\bar{q}}> / < n_g + n_q + n_{\bar{q}}> . \quad (7)$$

Then the strong coupling is given by the one-loop running coupling formula $\alpha_s(Q) = 4\pi/\beta_0 \ln(Q^2/\Lambda_{QCD}^2)$. We choose an average value $\Lambda_{QCD} = 235$ MeV [30] and $n_f = 2.5$. As already mentioned, this last approach eliminates the coupling as the remaining external parameter.

III. RESULTS AND DISCUSSIONS

We use the same initial conditions T_0 , l_{0i} , ϵ_{0i} , n_{0i} , where $i = g, q, \bar{q}$ as before [2] to compare with our previous results. One notes that these values from HIJING [31–33] have small initial fugacities which is partly responsible for the not-so-well quark chemical equilibration. One could try multiplying the initial fugacities by a factor to compensate for this as done in [34,35] and also recently in [36]. Here we concentrate only on the effects of the variation of α_s and not worry ourselves about the initial conditions.

Our plots are produced with $\alpha_s = 0.3, 0.5, 0.8, \alpha_s^v$. The last denotes the coupling which varies with the evolution according to the recipe given in the preceding section. To look at the effects of α_s on equilibration, we examine the parton fugacities l , the longitudinal to transverse pressure ratios p_L/p_T and then also the temperature estimates T of the each parton component of the plasma. The first give us information about the parton composition, the second reveal the state of the kinetic equilibration of the system and the last tell us about the possible lifetime of the parton plasma. In Fig. 2, Fig. 3 and Fig. 4, we plotted these results.

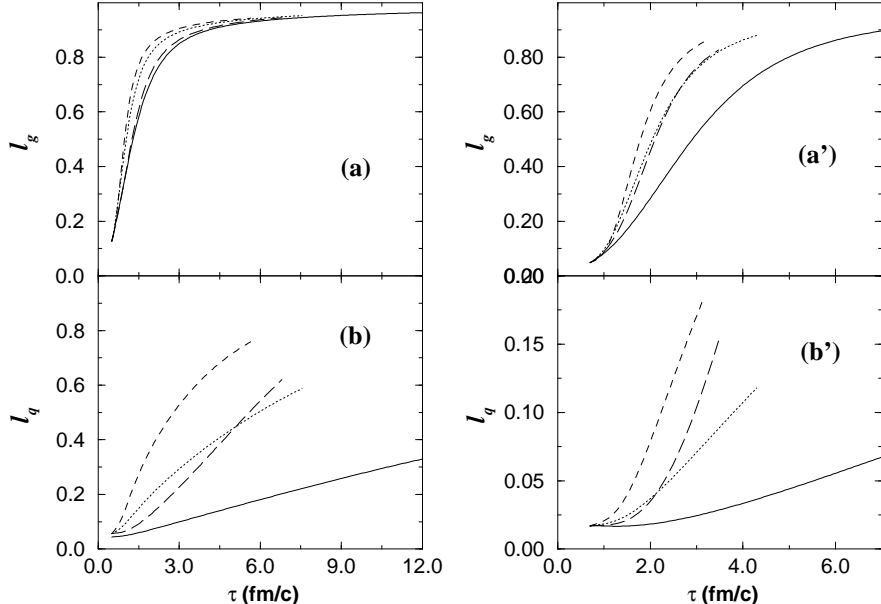


FIG. 2. Chemical equilibration of (a) gluons and (b) quarks with various values for the coupling: $\alpha_s = 0.3$ (solid), 0.5 (dotted), 0.8 (dashed) and α_s^v (long dashed) at LHC. The (a') and (b') figures are the same at RHIC. Increasing coupling improves the quark final degree of chemical equilibration much more than that of the gluon.

With varying α_s , the fugacity evolution is as in Fig. 2. The curves shift towards the upper left hand corner with increasing α_s . This is the same for gluons Fig. 2 (a) and (a') and for quarks Fig. 2 (b) and (b'). As can be seen, larger α_s leads to faster approach towards full chemical equilibration. Curves with larger α_s rise faster. For gluons, it takes less time to achieve approximately the same degree of chemical equilibration. Whereas for quarks, the final fugacities are improved by 1.5-2.0 times at LHC and a somewhat larger factor of 1.8-2.8 at RHIC. These enhancement factors clearly depend on how close to equilibrium the previous $\alpha_s = 0.3$ results are. When it is farther from 1.0 as in the fermion case at RHIC, the factors are largest and when it is close or very close as in the gluon case, there are

not much improvements. Or rather there is not much room for improvement because it cannot go further than full equilibration and the undoing effects of the back reactions are important at this stage of the equilibration. The effect of larger α_s is to shorten the lifetime of the parton phase of the plasma only in this case.

Similar situation is also found in the ratios of longitudinal to transverse pressure which is a check of isotropy of parton momentum distributions and a test of kinetic equilibration. In Fig. 3, we plot the pressure ratios p_L/p_T as well as $\epsilon/3p_T$ both for quarks (b) and (b') and for gluons (a) and (a') at LHC and at RHIC respectively. The top set of curves in each case is the $\epsilon/3p_T$ plots. In these plots, curves with larger α_s are closer to the top in general. In other words, they are closer to full kinetic equilibrium. As in the case of fugacities, kinetic equilibration is clearly faster as the amount of time required to reach the same or a higher degree of equilibration is shorter. However, the final situations for gluons are about the same. The improvements for quarks are again much clearer. Both p_L/p_T and $\epsilon/3p_T$ plots show the same tendency. It becomes obvious that increasing α_s improves the equilibration of quarks and antiquarks much more than that of the gluons. These improvements and faster equilibration are however at a price. One can see that the curves with larger couplings are stopped earlier and that is because the price to be paid is more rapid cooling for larger α_s . This can be seen more clearly in the plots of the estimated temperatures in Fig. 4.

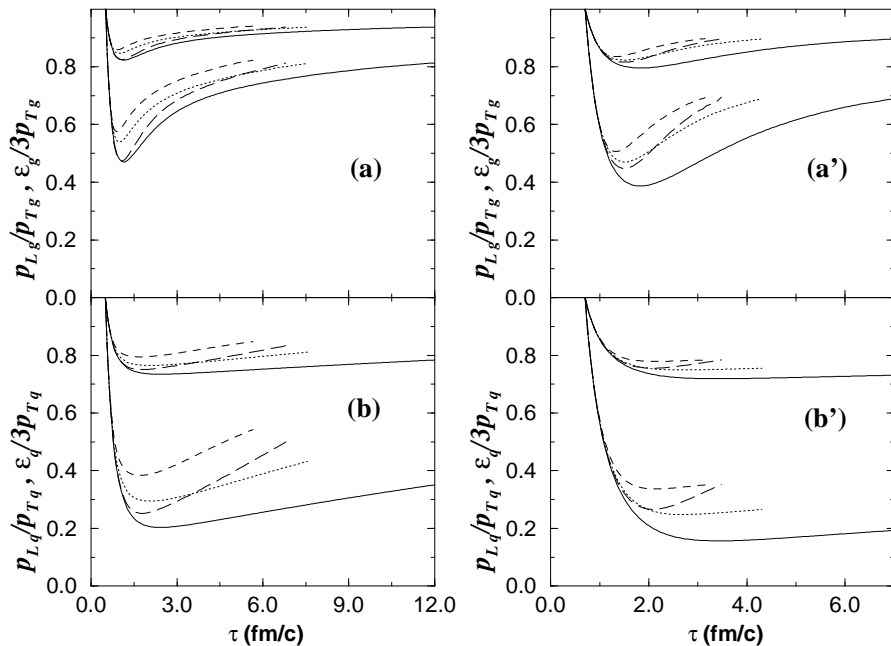


FIG. 3. Using the ratios of the longitudinal pressure and a third of the energy density to the transverse pressure to check for isotropy in momentum distribution and therefore kinetic equilibration. The bottom (top) set of four curves in each figure is for the pressure (energy density) to pressure ratio. The assignments of the coupling to the curves are $\alpha_s = 0.3$ (solid), 0.5 (dotted), 0.8 (dashed) and α_s^v (long dotted). Figures (a) and (a') are for gluons and (b) and (b') for quarks at LHC and at RHIC respectively. Faster kinetic equilibration is seen everywhere with larger α_s but improvement in the final degree of thermalization is essentially reserved for the fermions and not for the gluons.

One remarks from Fig. 4, that the effect on the lifetime is considerable as a shift from $\alpha_s = 0.3$ to 0.5 shortens the time at which the quark temperatures drop to 200 MeV from 12.0 fm/c to 8.4 fm/c at LHC in Fig. 4 (b) and from 7.0 fm/c to 4.3 fm/c at RHIC in Fig. 4 (b'). The reduction on this same duration of the gluon temperatures is less and is only about 2.0 fm/c at LHC in Fig. 4 (a) and 1.0 fm/c at RHIC in Fig. 4 (a') at maximum. Although gluons always cool faster than quarks due to the combined effects of the expansion and the loss of gluons to quarks and antiquarks, the cooling of the fermions are, like the fugacities and pressure ratios, affected more by the coupling. In all, the duration of the parton phase of the plasma is very sensitive to the value of the coupling. To have to choose a value of the coupling by hand is almost equivalent to choosing the results. So it may be more consistent by the arguments already given to let the system determines its strength of the interactions.

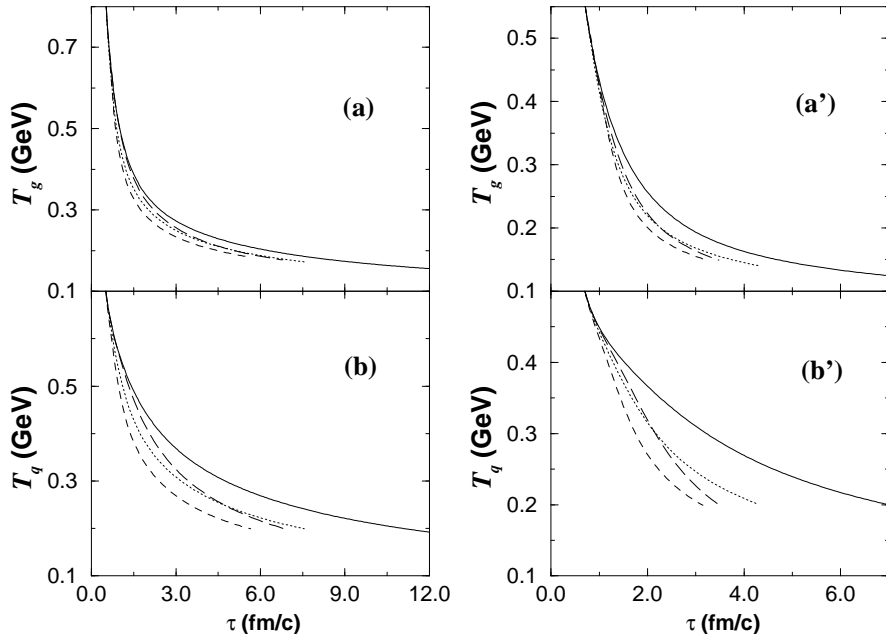


FIG. 4. The time variations of the estimated temperatures of (a) and (a') gluons and (b) and (b') quarks at LHC and at RHIC respectively. These temperatures drop faster with increasing coupling. The different values of the coupling are assigned to the curves in the same way as in Fig. 2 and Fig. 3.

For the reasons discussed in Sec. I and in the previous paragraph, the case of α_s evolving with the system, α_s^v , interests us particularly. In the plots Fig. 2, Fig. 3 and Fig. 4, these curves shift across the constant α_s “contours” with increasing τ . Since the strength of the interactions changes with the evolution, the results are progressive departures from the previous and they improve progressively upon those in the sense that the fugacities, the pressure ratios are larger and therefore closer to equilibrium at the expense of more rapid cooling and shortened lifetime. Since α_s^v shifts towards larger values of α_s , higher order terms will have to be included at some stage and eventually the problem will become non-perturbative. In this work, we try not to worry about higher orders and just examine the results at leading order.

We have seen the results of how α_s affects the approach to equilibrium. They tell us about chemical and kinetic equilibration are speeded up and the final degrees of these two aspects of equilibration have been altered but they do not tell us much about how the partons are behaving with increasing coupling. In this sense, collective variables are much more suitable for this purpose. In any case, it would be interesting also to see how the collective variables are affected by the coupling.

In Fig. 5, the variation of the products of the parton energy density ϵ_i with $\tau^{4/3}$ are plotted. It would be helpful to think of each parton component of the plasma to be subjected to an effective longitudinal pressure $p_{L\text{eff}}$, so that the equations for the energy densities, which follow from Eq. (1) and (2) [2], become

$$\frac{d\epsilon_i}{d\tau} + \frac{\epsilon_i + p_{L\text{eff}}}{\tau} = 0 \quad (8)$$

with the effective pressures given by

$$p_{L\text{eff}} = p_{L\text{i}} + \frac{\tau(\epsilon_i - \epsilon_{eq\text{i}})}{\theta_i} . \quad (9)$$

In Fig. 5 (a) and (a'), the effective pressure of the gluons tends to increase with α_s and be larger than one-third of the gluon energy density hence the decreasing tendency of $\epsilon_i \tau^{4/3}$. The opposite is true for the quark effective pressure in Fig. 5 (b) and (b'). In Fig. 3, we have already seen that the longitudinal pressures for all partons are less than a third of the corresponding energy density so the second term in Eq. (9) must be positive (negative) and increasing (decreasing) with the coupling for gluons (quarks). In other words, the net energy transfer from gluons to quarks and antiquarks is positive and increasing with α_s . This variation in the net energy transfer is accompanied by a corresponding increase in the loss of gluon number and gluon entropy and similarly an increase in the gain of quark-antiquark pairs and quark entropy. These are shown in Fig. 6 and Fig. 7.

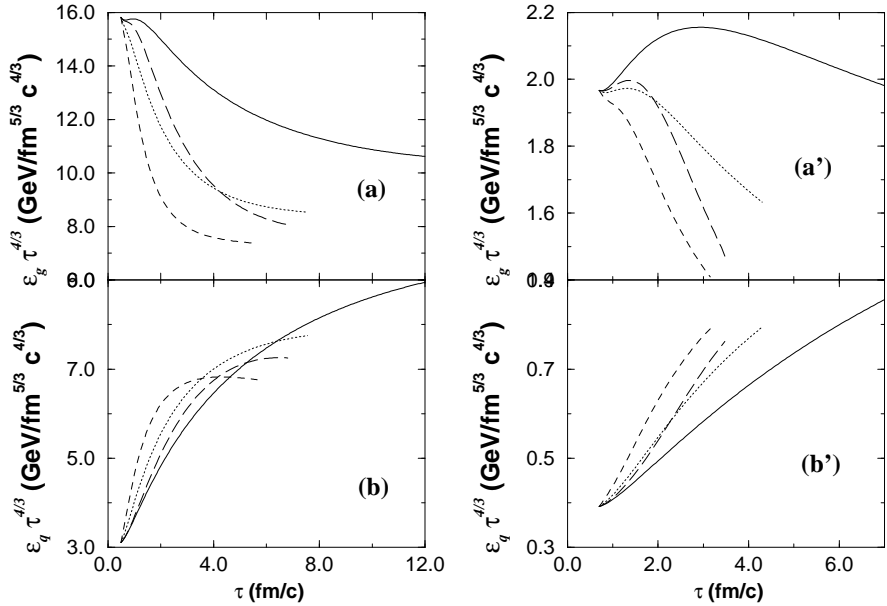


FIG. 5. From the products $\epsilon_i \tau^{4/3}$, one can deduce information on the effective pressure $p_{L,i \text{ eff}}$ and hence the energy transfer variation with the coupling. As before (a) and (b) are results for LHC and (a') and (b') are those for RHIC. The couplings are assigned to the curves in the same way as in previous figures.

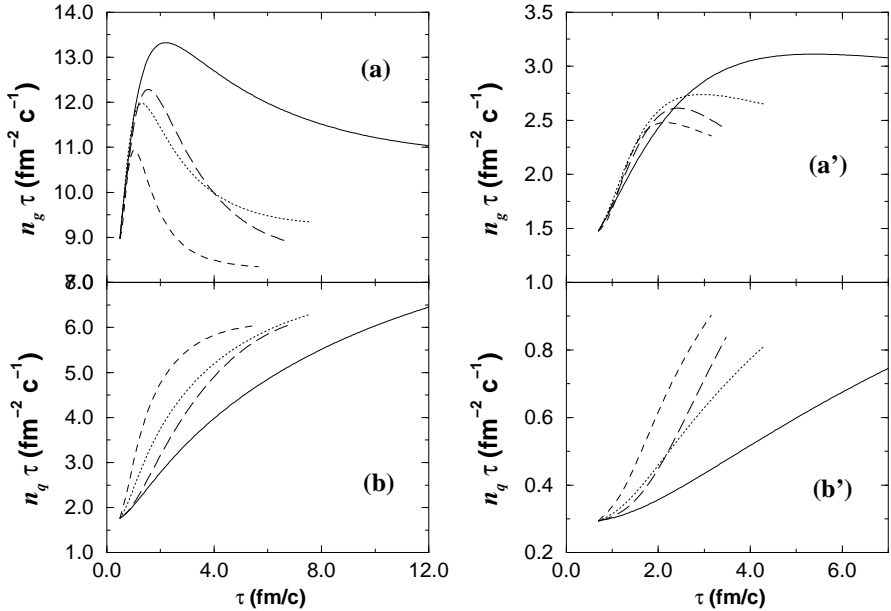


FIG. 6. These figures show the more favorable conversion of gluons into quark-antiquark pairs with increasing coupling. The reduction in the produced net number of gluons in (a) and (a') and therefore the diminution of the gluon density is accompanied by the more abundance creation of fermion pairs shown in (b) and (b') and hence an increase of their density.

The net creations of gluons are reduced more and more with increasing α_s in Fig. 6 (a) and (a') by the stronger conversion process of gluons into quark-antiquark pairs in Fig. 6 (b) and (b'). As seen, these result in the lowering and earlier occurring of the peak number of gluons in figure (a) and (a') and the drop in gluon density is accompanied by an increase in the quark and antiquark density. This is so because of the faster chemical equilibration which we have already seen with increasing coupling so gluons are closer to chemical equilibrium earlier which favors the conversion into quark-antiquark pairs.

The last collective variable and also the most important one that we are interested in is the entropy. As we have already mentioned, in Fig. 7, one can see the product of the gluon entropy density s_g with τ , $s_g \tau$, for various α_s

decreases faster and just the opposite happens to the product $s_q\tau$. They increase more rapidly with α_s . These are as expected from the results obtained so far. The most interesting part is however in the product of the total entropy density with τ . The more rapid equilibration associated with larger α_s reduces the produced entropy and therefore final pion multiplicity when the plasma eventually freezes and breaks up. This is most clear at LHC where the state of equilibration is much better than that at RHIC.

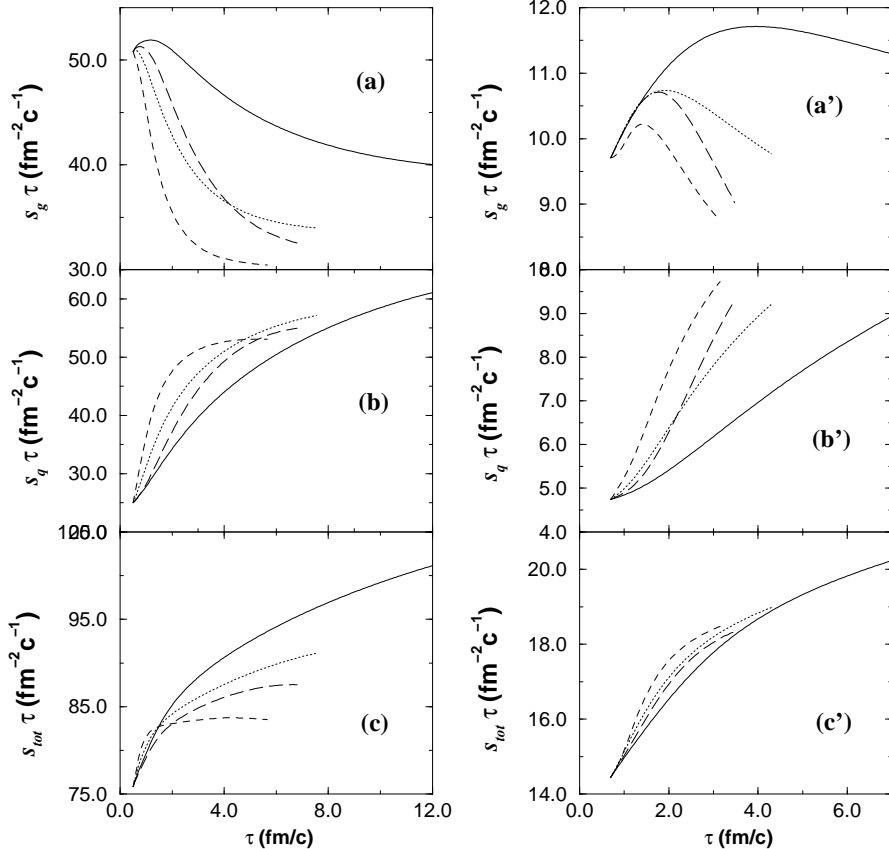


FIG. 7. Whereas there is an increasing gain in the quark and antiquark entropy with increasing coupling in (b) and (b'), the gluon entropy is reduced more and more in (a) and (a'). The total sum is also reduced by increasing strength of the interactions. This is much clearer at LHC in (c) where the state of the equilibration is much better than that at RHIC in (c').

From these last discussed figures, one can again see the faster equilibration with increasing α_s already shown in Fig. 2 and Fig. 3. As discussed in some details in [2], energy transfer and number conversion between gluons and quarks and antiquarks will tend to zero as equilibrium is approached, therefore the products in Fig. 5 and Fig. 6 will tend to be independent of τ . Also entropy generation will cease once equilibrium has been attained, then the product in Fig. 7 will likewise progressively be independent of τ . At LHC, one can see this quite clearly but unfortunately not so at RHIC.

In [1,2], we have discussed the connection of the collision time θ with the stage of the equilibration. A large θ indicates a small net interaction rate and *not* a small interaction rate since it is the difference between the forward and backward reaction which enters the collision terms in the Boltzmann equation. Due to colour, quark and antiquark interact more weakly than gluon in general, therefore $\theta_g < \theta_q$. With our initial conditions, interactions have to bring the expanding plasma under control first before guiding it towards equilibrium. This is manifested in the initial rapid drop of θ , especially θ_q , and the eventual slow rise. The initial rapid drop in θ is a response of the system to being driven out of equilibrium by the expansion. The net interaction rate is forced to increase rapidly until it overtakes the expansion rate, at which point θ ends its downward descent and begins its slow rise. With close to equilibrium initial conditions, the initial drop will be absent. One can understand the final behavior from the calculations of relaxation time near equilibrium [37–39]. Their known behavior near equilibrium is $1/T$ so as the system cools, the collision time should rise. In terms of the net interaction rate, this rate will become slower and slower as equilibrium is near so θ must rise. This behavior is correct has already been demonstrated in [1]. One can see from Fig. 8 (a) and (b) for both θ_g and θ_q at LHC and similarly in the (a') and (b') figures at RHIC, the same patterns appear in all the fixed

α_s results. But for the α_s^v case, something very interesting happens. The later stage increase with τ of θ_g is either less fast for the gluons in (a) or in (a') and for the quarks θ_q in (b) and (b'), where they even decrease further with τ . This continued decrease is however different from the initial rapid drop and it does not mean that the plasma is not approaching equilibrium according to our reasoning given here. As we saw in Fig. 2 and Fig. 3, this is not the case but rather α_s^v evolves in such a way as to compensate for the slowing down of the net interaction rate as equilibrium is approached. This only happens in a non-abelian theory with asymptotic freedom as in the case of QCD. It does not happen if the strength of the interaction is fixed as in an usual ideal molecular gas for example. So the equilibration of the parton plasma is helped along the way towards equilibrium by the increasing coupling but this same phenomena will cut short the equilibration of the parton system as the deconfinement phase transition begins to take place. In the case of a first order phase transition, the equilibration will continue in the mixed hadron-parton system and is outside the scope of this paper.

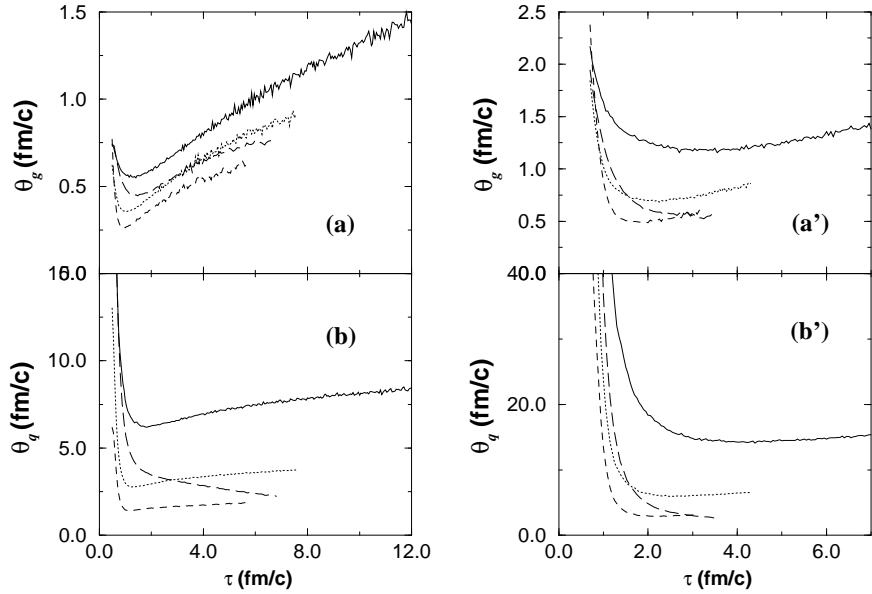


FIG. 8. The time evolution of the collision time reflects the state of the equilibration. The behaviors are similar amongst the curves with constant couplings: $\alpha_s = 0.3$ (solid), 0.5 (dotted) and 0.8 (dashed). The exceptions are the curves with the varying coupling α_s^v (long dashed) both at LHC (a) and (b) and at RHIC (a') and (b') which show accelerated approach to equilibrium not found in the equilibration of ordinary many-body system.

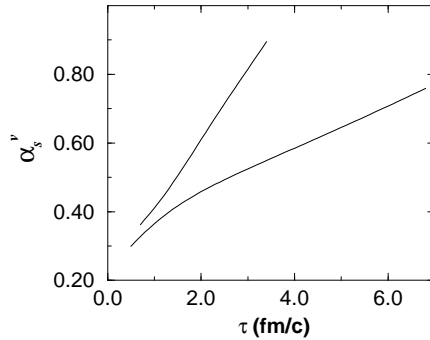


FIG. 9. As the expanding parton plasma approaches equilibrium, the strength of the interactions also increases which is the basic reason for the acceleration in the equilibration. As seen here, perturbative calculations are less favorable at RHIC (top curve) than at LHC (bottom curve).

Finally, we plot the evolution of α_s^v in Fig. 9. The bottom (top) curve is for LHC (RHIC). The values of α_s^v depend to a certain extent on the Λ_{QCD} used. With our present choice, RHIC is seen to be less favorable for perturbative calculations than LHC. Because α_s^v never exceeds 1.0, one can still use perturbative calculation in principle. However the values of α_s^v at later stages are uncomfortably large. At some point already higher orders have better be included.

How these will alter our results will have to be studied. Since initial conditions from HIJING used here are, perhaps, some of the less favorable inputs, one can envisage other ones that could prolong the duration favorable for perturbative calculations.

To summarize, we have checked how equilibration is affected by the choice of the coupling and we have also shown that to use a fixed value of the coupling for the whole duration of the parton plasma right down to the deconfinement phase transition is not consistent. The results of the equilibration do depend on what α_s is used. In particular, the duration of the parton phase and the entropy are sensitive to the value of α_s . Between gluons and quarks, only the quark final degree of equilibration is affected by the value of the coupling. So, in general, to let the system decides its own strength of the interactions may be a better choice. The best choice is then not to have to choose at all. With a evolving coupling, equilibration is faster and better because the now increasingly strongly interacting parton plasma compensates for the slowing down of the equilibration as equilibrium is approached. This accelerated approach to equilibrium is not found in other many-body system and is unique to the parton plasma in which the interactions are described by the QCD Lagrangian. Because the gluon end degree of equilibration does not change much with the coupling but that of the quark does, the second stage in the two-stage equilibration scenario [40] will not last as long as with a fixed coupling at $\alpha_s = 0.3$, if the phase transition has not already started before its completion.

ACKNOWLEDGEMENTS

The author would like to thank Al Mueller for giving the idea to this investigation and for discussion.

- [1] S.M.H. Wong, Nucl. Phys. A **607**, 442 (1996).
- [2] S.M.H. Wong, Phys. Rev. C **54**, 2588 (1996).
- [3] K. Geiger and B. Müller, Nucl. Phys. B **369**, 600 (1991).
- [4] K. Geiger, Phys. Rev. D **46**, 4965, 4986 (1992).
- [5] K. Geiger and J.I. Kapusta, Phys. Rev. D **47**, 4905 (1993).
- [6] T.S. Biró, E. van Doorn, B. Müller, M.H. Thoma and X.N. Wang, Phys. Rev. C **48**, 1275 (1993).
- [7] K.J. Eskola, Nucl. Phys. A **590**, 1995 (383c).
- [8] A.H. Weldon, Phys. Rev. D **26**, 1394,2789 (1982).
- [9] V.V. Klimov, Yad. Fiz. **33**, 1734 (1981), Sov. J. Nucl. Phys. **33**, 934 (1981).
- [10] E.V. Shuryak and L. Xiong, Phys. Rev. C **49**, 2203 (1994).
- [11] J. Winter, J. Phys. (Paris) Colloq. **45**, C6-53 (1984).
- [12] U. Heinz, Phys. Rev. Lett. **51**, 351 (1983).
- [13] H.Th. Elze, M. Gyulassy and D. Vasak, Nucl. Phys. B **276**, 706 (1986); Phys. Lett. B **177**, 402 (1986).
- [14] H.Th. Elze and U. Heinz, Phys. Rep. **183**, 81 (1989).
- [15] H.Th. Elze, Z. Phys. C **47**, 647 (1990).
- [16] H. Weigert and U. Heinz, Z. Phys. C **50**, 195 (1991).
- [17] U. Heinz, Proceedings of the Banff/CAP Workshop on Thermal Field Theories, F.C. Khanna et al., eds., World Scientific 1994, p.428.
- [18] S. de Groot, W.A. van Leuwen, and C.G. van Weert, Relativistic Kinetic Theory, North-Holland, Amsterdam (1980).
- [19] G. Baym, Phys. Lett. B **138**, 18 (1984).
- [20] H. Heiselberg and X.N. Wang, Nucl. Phys. B **462**, 389 (1996).
- [21] S. Gavin, Nucl. Phys. B **351**, 561 (1991).
- [22] K. Kajantie and T. Matsui, Phys. Lett. B **164**, 373 (1985).
- [23] H. Heiselberg and X.N. Wang, Phys. Rev. C **53**, 1892 (1996).
- [24] R. Cutler and D. Sivers, Phys. Rev. D **17**, 196 (1978).
- [25] M. Gyulassy and X.N. Wang, Nucl. Phys. B **420**, 583 (1994).
- [26] M. Gyulassy, M. Plümer and X.N. Wang, Phys. Rev. D **51**, 3436 (1995).
- [27] R. Baier, Yu.L. Dokshitser, S. Peigné and D. Schiff, Phys. Lett. B **345**, 277 (1995).
- [28] St. Mrówozynski, Phys. Rev. C **49**, 2191 (1994).
- [29] St. Mrówozynski, preprint hep-ph/9606442.
- [30] R.M. Barnett et al, Phys. Rev. D **54**, 1 (1996).
- [31] M. Gyulassy and X.N. Wang, Phys. Rev. D **44**, 3501 (1991).
- [32] M. Gyulassy, M. Plümer, M. Thoma and X.N. Wang, Nucl. Phys. A **538**, 37c (1992).

- [33] M. Gyulassy and X.N. Wang, Nucl. Phys. A **544**, 559c (1992).
- [34] P. Lévai, B. Müller and X.N. Wang, Phys. Rev. C **51**, 3326 (1995).
- [35] X.N. Wang, Nucl. Phys. A **590**, 47 (1995).
- [36] B. Müller, M.G. Mustafa, D.K. Srivastava, preprint nucl-th/9611041.
- [37] G. Baym, H. Monien, C.J. Pethick and D.G. Ravenhall, Nucl. Phys. A **525**, 415c (1991).
- [38] G. Baym, H. Heiselberg, C.J. Pethick and J. Popp, Nucl. Phys. A **544**, 569c (1992).
- [39] H. Heiselberg, Phys. Rev. Lett. **72**, 3013 (1994).
- [40] E.V. Shuryak, Phys. Rev. Lett. **68**, 3270 (1992).

FIGURE CAPTIONS

Fig. 1 The evolution of the average parton energy of gluon (solid line) and quark or antiquark (dashed line) at (a) LHC and (b) RHIC with $\alpha_s = 0.3$.

Fig. 2 Chemical equilibration of (a) gluons and (b) quarks with various values for the coupling: $\alpha_s = 0.3$ (solid), 0.5 (dotted), 0.8 (dashed) and α_s^v (long dashed) at LHC. The (a') and (b') figures are the same at RHIC. Increasing coupling improves the quark final degree of chemical equilibration much more than that of the gluon.

Fig. 3 Using the ratios of the longitudinal pressure and a third of the energy density to the transverse pressure to check for isotropy in momentum distribution and therefore kinetic equilibration. The bottom (top) set of four curves in each figure is for the pressure (energy density) to pressure ratio. The assignments of the coupling to the curves are $\alpha_s = 0.3$ (solid), 0.5 (dotted), 0.8 (dashed) and α_s^v (long dotted). Figures (a) and (a') are for gluons and (b) and (b') for quarks at LHC and at RHIC respectively. Faster kinetic equilibration is seen everywhere with larger α_s but improvement in the final degree of thermalization is essentially reserved for the fermions and not for the gluons.

Fig. 4 The time variations of the estimated temperatures of (a) and (a') gluons and (b) and (b') quarks at LHC and at RHIC respectively. These temperatures drop faster with increasing coupling. The different values of the coupling are assigned to the curves in the same way as in Fig. 2 and Fig. 3.

Fig. 5 From the products $\epsilon_i \tau^{4/3}$, one can deduce information on the effective pressure $p_{L\,i\,\text{eff}}$ and hence the energy transfer variation with the coupling. As before (a) and (b) are results for LHC and (a') and (b') are those for RHIC. The couplings are assigned to the curves in the same way as in previous figures.

Fig. 6 These figures show the more favorable conversion of gluons into quark-antiquark pairs with increasing coupling. The reduction in the produced net number of gluons in (a) and (a') and therefore the diminution of the gluon density is accompanied by the more abundance creation of fermion pairs shown in (b) and (b') and hence an increase of their density.

Fig. 7 Whereas there is an increasing gain in the quark and antiquark entropy with increasing coupling in (b) and (b'), the gluon entropy is reduced more and more in (a) and (a'). The total sum is also reduced by increasing strength of the interactions. This is much clearer at LHC in (c) where the state of the equilibration is much better than that at RHIC in (c').

Fig. 8 The time evolution of the collision time reflects the state of the equilibration. The behaviors are similar amongst the curves with constant couplings: $\alpha_s = 0.3$ (solid), 0.5 (dotted) and 0.8 (dashed). The exceptions are the curves with the varying coupling α_s^v (long dashed) both at LHC (a) and (b) and at RHIC (a') and (b') which show accelerated approach to equilibrium not found in the equilibration of ordinary many-body system.

Fig. 9 As the expanding parton plasma approaches equilibrium, the strength of the interactions also increases which is the basic reason for the acceleration in the equilibration. As seen here, perturbative calculations are less favorable at RHIC (top curve) than at LHC (bottom curve).